

Implementation of anisotropic soft pads in a surgical gripper for secure and gentle grip on vulnerable tissues

van Assenbergh, Peter; Culmone, Costanza; Breedveld, Paul; Dodou, Dimitra

DOI

[10.1177/0954411920971400](https://doi.org/10.1177/0954411920971400)

Publication date

2021

Document Version

Final published version

Published in

Proceedings of the Institution of Mechanical Engineers, Part H: Journal of Engineering in Medicine

Citation (APA)

van Assenbergh, P., Culmone, C., Breedveld, P., & Dodou, D. (2021). Implementation of anisotropic soft pads in a surgical gripper for secure and gentle grip on vulnerable tissues. *Proceedings of the Institution of Mechanical Engineers, Part H: Journal of Engineering in Medicine*, 235(3), 255-263.
<https://doi.org/10.1177/0954411920971400>

Important note

To cite this publication, please use the final published version (if applicable).
Please check the document version above.

Copyright

Other than for strictly personal use, it is not permitted to download, forward or distribute the text or part of it, without the consent of the author(s) and/or copyright holder(s), unless the work is under an open content license such as Creative Commons.

Takedown policy

Please contact us and provide details if you believe this document breaches copyrights.
We will remove access to the work immediately and investigate your claim.

Green Open Access added to TU Delft Institutional Repository

'You share, we take care!' - Taverne project

<https://www.openaccess.nl/en/you-share-we-take-care>

Otherwise as indicated in the copyright section: the publisher is the copyright holder of this work and the author uses the Dutch legislation to make this work public.

Implementation of anisotropic soft pads in a surgical gripper for secure and gentle grip on vulnerable tissues

Peter van Assenbergh*^{ID}, Costanza Culmone*^{ID},
Paul Breedveld and Dimitra Dodou^{ID}

Proc IMechE Part H:
J Engineering in Medicine
1–9

© IMechE 2020

Article reuse guidelines:

sagepub.com/journals-permissions

DOI: 10.1177/0954411920971400

journals.sagepub.com/home/pih



Abstract

Current surgical grippers rely on friction grip, where normal loads (i.e. pinch forces) are translated into friction forces. Operating errors with surgical grippers are often force-related, including tissue slipping out of the gripper because of too low pinch forces and tissue damaging due to too high pinch forces. Here, we prototyped a modular surgical gripper with elastomeric soft pads reinforced in the shear direction with a carbon-fiber fabric. The elastomeric component provides low normal stiffness to maximize contact formation without the need of applying high normal loads (i.e. pinch forces), whereas the carbon-fiber fabric offers high shear stiffness to preserve the formed contact under the lateral loads (i.e. shear forces) that occur during tissue lifting. Additionally, we patterned the pads with a sub-surface micropattern, to further reduce the normal stiffness and increase shear stiffness. The body of the prototype gripper, including shaft, joints, and gripper tips, was fabricated in a single step using 3D printing, followed by manual attachment of the soft pads to the gripper. The gripping performance of the newly developed soft gripper on soft tissues was experimentally compared to reference grippers equipped with metal patterned pads. The soft-pad gripper generated similar gripping forces but significantly lower pinch forces than metal-pad grippers. We conclude that grippers with anisotropic-stiffness pads are promising for secure and gentle tissue grip.

Keywords

Surgical gripper, soft pads, anisotropic stiffness

Date received: 30 May 2020; accepted: 12 October 2020

Introduction

Secure and gentle soft-tissue grip is imperative in the medical domain. In almost any surgical procedure, from laparoscopy to microsurgery, soft tissues are grasped and pulled for creating space, exposing areas to be treated, or getting access to obstructed contiguous anatomical structures. The vast majority of surgical grippers used in the medical domain are equipped with patterned surfaces made of stainless steel.¹ Such grippers employ friction grip, which relies on the translation of normal load (i.e. pinch forces) to friction forces, for grasping and pulling soft tissues.

Previous studies have shown that the majority of grasping errors with surgical grippers is force-related, with pinch forces being either too low, resulting in slipping of the tissue out of the gripper,^{2,3} or too high, resulting in possible tissue damage.^{4,5} Tissue stresses up to 800 kPa have been measured with laparoscopic grippers,⁶ which is considerably higher than the safety threshold of 200 kPa estimated for apoptosis.⁷

Studies have shown that high pinch forces can be reduced by replacing the metal forceps of the gripper with soft pads.^{8,9} The grip of such pads on tissue is achieved thanks to their deformability in the normal direction, which enables a large contact area with the tissue. At the same time, the contact formed between the tissue and the pad is homogeneously distributed over the pad surface, eliminating the occurrence of local high peak forces on the tissue.^{8,9} A general disadvantage of a soft pad is that deformations of the pad

Department of Biomechanical Engineering, Delft University of Technology, Delft, Zuid-Holland, The Netherlands

* Peter van Assenbergh and Costanza Culmone contributed equally to the manuscript

Corresponding author:

Peter van Assenbergh, Department of Biomechanical Engineering, Delft University of Technology, Mekelweg 2, Delft, Zuid-Holland 2628CD, The Netherlands.

Email: s.p.vanassenbergh@tudelft.nl

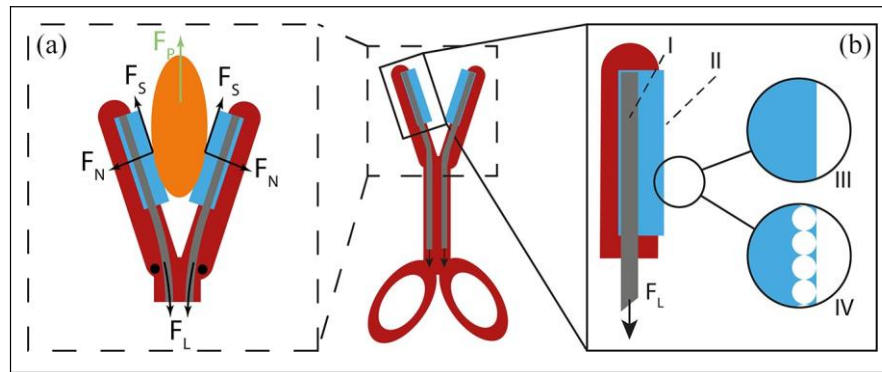


Figure 1. A schematic overview of a gripper pad with anisotropic properties: (a) schematic force diagram. Hinges are depicted as black dots. The gripper was closed by loading the CFF using a constant tensile load (F_L). By closing the gripper, the pinch force (F_N) acts on the tissue in the normal direction. When the tissue sample was pulled upwards using a positioning stage (F_p), a shear force (F_S) was generated at the soft pad-tissue interface. Gravitational force on the tissue is omitted from the diagram because the load cell to which the tissue was connected via a holder (not visualized here) was zeroed after the tissue was hung to the holder and (b) a stiff carbon-fiber fabric (CFF) (I) is partially embedded into a soft elastomeric material (PDMS) (II). The CFF is aligned with the shear (pulling) direction. The loading forces are guided via the unembedded CFF tail into the shaft of the instrument. The pad is fabricated either without a surface pattern (III) or with a pattern of microscale sub-surface spherical voids (IV). Under shear loading, the internal walls that separate neighboring voids collapse, resulting in lateral stiffening of the adhesive surface.

occur not only in the normal but also in the shear direction, which might lead to tissue slipping out of the gripper during pulling. An ideal soft gripping pad would thus need to be anisotropic, fulfilling two contradictory properties: being deformable in the normal (pinching) direction, so that a large contact is formed, and stiff in the lateral (shear) direction, so that the formed contact is preserved when the tissue is being pulled.

Bartlett et al.¹⁰ developed such anisotropic pads for strong grip on rigid substrates. The pads consisted of a carbon-fiber fabric (CFF), part of which was embedded into an elastomeric material (poly-dimethylsiloxane, PDMS); the unembedded CFF part was served as tail via which the pad was pulled along the substrate. PDMS provided deformability in the normal direction, thereby allowing for the formation of a large contact, whereas CFF provided stiffness in the shear direction, thus allowing for the preservation of the formed contact when pulling the pad from the CFF tail along the substrate. These authors found that, on rigid glass substrates, 100 cm² elastomeric pads without CFF had a force capacity (i.e. maximum sustainable force) of about 10 N, whereas the addition of CFF led to a force capacity in the order of 1000 N.¹⁰

Implementation of anisotropic CFF-PDMS pads in surgical grippers is a promising approach for generating secure, yet gentle, grip on biological tissue. The idea herein is to align the CFF with the shear (pulling) direction and guide the loading forces via the CFF tail into the shaft of the instrument in such a way that the elastomeric part of the soft pad is protected from undesirable shear deformations and contact loss (Figure 1).

The grip of fiber-reinforced soft pads can be further increased by patterning the otherwise plain surface of the elastomer (Figure 1). In previous work, we showed that, on soft substrates, the presence of microscale

spherical voids in an elastomer, topped with a thin terminal layer, led to higher grip than an unpatterned elastomer.¹¹ Thanks to its microscale thickness, the terminal layer conforms to microscale irregularities of the substrate's surface, resulting in a higher contact area compared to an unpatterned elastomer, and therefore higher shear forces. At the same time, due to bending and internal sliding of the walls that separate the internal spherical voids under shear loading, the surface structure of the elastomer stiffens in the shear direction, thereby contributing to the preservation of the formed contact during shearing.^{11,12}

In this paper, we present the implementation of fiber-reinforced elastomeric soft pads in a modular surgical gripper instrument. We developed two types of fiber-reinforced soft pads, one with an unpatterned surface, and another with sub-surface microscale voids. Additionally, we fabricated a reference gripper by replacing the pads with stainless steel grooved plates. The performance of the three grippers on soft tissue was assessed by measuring their gripping and pinch forces applied to the tissue.

Design Soft pads

Unpatterned soft pads were fabricated with a thickness of 0.8 mm, width of 8 mm, and length of 15 mm. A piece of polystyrene plastic foil (50 \times 50 mm²), acting as an anti-stick layer, was placed on an aluminum base plate (Figure 2(a)). This anti-stick layer was covered with a 200 \times 50 mm² piece of CFF (Figure 2(b); 3K-200 Tex HS fibers, 200 gr/m², plain woven, purchased from www.carbonwinkel.nl, De Moer, the Netherlands), which was fixed at the short side of the baseplate using

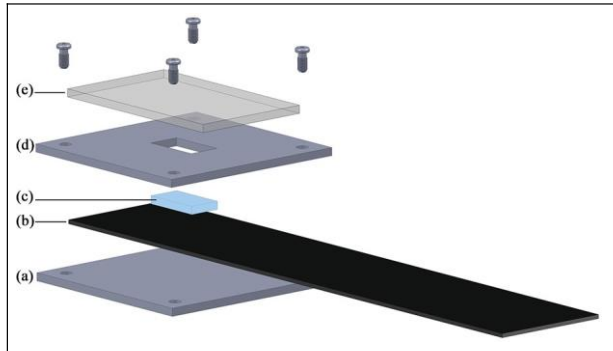


Figure 2. Exploded view of soft pad fabrication. An aluminum baseplate, topped with an anti-stick polystyrene foil (a) was covered with a sheet of CFF (b). A template frame in the size and thickness of the envisioned soft pad (d) was placed on the CFF and filled with uncured PDMS (c). The filled frame was covered with a plain or coated glass slide (e) to obtain unpatterned or patterned pads after curing.

scotch tape. An $83 \times 15 \text{ mm}^2$ rectangular hole was milled from an aluminum plate of 0.8 mm thickness to create a template frame (Figure 2(d)). Sylgard-184 (PDMS, purchased from Dow Corning, MI) pre-polymer (base) and crosslinker (curing agent) were mixed in a 10:1 weight-based mixing ratio and degassed in a desiccator. The template frame was placed on top of the aluminum base plate covered with CFF and filled with the pre-polymer/crosslinking mixture. The filled template frame was degassed once more to evacuate air from the CFF, allowing the pre-polymer/crosslinking mixture to fully immerse the CFF. After degassing, the filled template was cured at 70°C for at least 2 h, while topped with a plain glass slide to obtain a flat finish (Figure 2(e)). After curing, the soft pad was carefully detached from the frame, anti-stick layer, and topping glass slide. The non-immersed CFF was cut to obtain two lateral flaps and a loading tail (Figure 2).

To fabricate patterned elastomeric pads, the aforementioned plain glass slide used to top the filled template after degassing was replaced by a coated glass slide to obtain a patterned finish of the soft pad. Thereto, a plain glass slide was coated with a colloidal monolayer, prepared using a dip-coating methodology, as described in earlier work.¹¹ In brief, styrene divinyl- benzene beads (purchased from ThermoFisher Scientific, MA, USA) with a reported diameter of 10 nm and delivered as a 4% (w/v) dispersion in water, were re-dispersed in ethanol at 8% (w/v) before use. The particles were transferred to the surface of a water bath, and compressed to obtain a closely packed floating monolayer of particles. In a dip-coating procedure, the monolayer was transferred to glass slides of $52 \times 76 \text{ mm}^2$. An initial dipping depth of at least 40 mm was used, resulting in monolayers with at least a $52 \times 40 \text{ mm}^2$ area. After curing of the soft PDMS pads, while topped with a coated glass slide, the microparticles were embedded in the pad

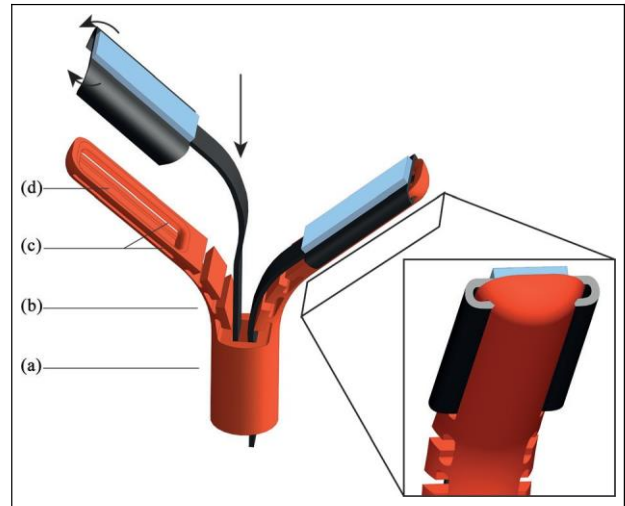


Figure 3. Schematic illustration of the gripper design for soft pads, and the positioning of the pads into the gripper. The shaft (a) contained a rectangular lumen, guiding the CFF to the joints. The flexural joints (b) were by default open, and straightened by pulling the CFF, resulting in closing of the gripper. Each jaw contained two lateral grooves (c) for fixation of the soft pads. The lateral CFF flaps of the soft pads were folded and glued into these grooves. Underneath the soft pads' center was an open space between jaw and soft pad (d), providing some mobility in the normal direction of the soft pad. The 3D printed gripper for metal pads differed from the grippers for soft pads, in that jaws had a flat surface upon which the metal pads were glued.

surface. Removing the microparticles was done by dissolving them in *n*-methyl-pyrrolidone (NMP, Merck, Darmstadt, Germany). Thereto, the pads were placed horizontally, with the pattern facing up, and a droplet of NMP, large enough to fully cover the pad surface, was deposited for a duration of 10 min, before it was rinsed off with ethanol. This washing step was repeated two more times. Pads for reference grippers were milled from stainless-steel with a triangular saw-tooth profile with 0.35 mm tooth height. The height of this surface pattern was chosen based on previous studies, which tested laparoscopic grippers with pattern depths varying between 0.3 and 1 mm^{13–15} and showed that a profile of 0.3 mm generated lower peak forces and thus less damage to the tissue.¹⁴

3D printed gripper

Figure 3 shows a schematic illustration of the 3D printed gripper, consisting of a shaft, joints, and jaws. Each gripper was 3D printed as a single element, and soft pads or reference pads were implemented in a subsequent manufacturing step. The grippers were printed using a Perfactory[®] 4 Mini XL printer (EnvisionTEC[®] GmbH, Gladbeck, Germany) with a layer height in the vertical *z*-axis of 25 μm. The selected printer is based on vat photopolymerization technology and uses

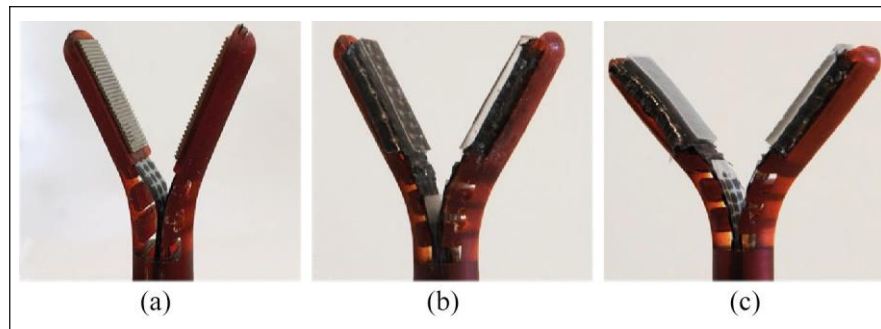


Figure 4. The three fabricated grippers. The reference gripper (a) was equipped with a grooved stainless-steel plate. In unpatterned pads (b), the elastomeric pads appear transparent, whereas in patterned pads (c), a white haze can be seen at the pad surface. In soft pads, either patterned or unpatterned, the CFF was embedded in the elastomeric pad.

Digital Light Processing (DLP), in which the build plate moves vertically up and down into a vat of liquid polymer. When the build plate moves down, the liquid polymer is exposed to light, and, depending on the image displayed by a projector, a layer of polymer hardens. The process is repeated layer-by-layer until the object is fully printed. The grippers were printed using R5 epoxy photopolymer resin (EnvisionTEC® GmbH, Gladbeck, Germany), an acrylic resin especially developed for prototyping. The 3D printed grippers were printed in 8 h, with a vertical orientation (i.e. the shaft in a vertical position, and the jaws pointing down).

The gripper shaft contained a central rectangular lumen to guide the CFF tail (Figure 3(a)). The flexural joints were based on a leaf-spring principle and printed in opened condition. The CFF tails were used to actuate the gripper; pulling them resulted in the straightening of both joints via elastic deformation, and closing of the jaws. For the fixation of the soft pads (unpatterned and patterned) to the 3D printed structure, two grooves were added on the long sides of each jaw (Figure 3(c)). The two lateral flaps of the CFFs were folded into the grooves and fixated by gluing with cyanoacrylate. The distal end was left free, and at the joint side of the pad, the CFF tail was guided into the shaft via the joint. Some open space was left between the soft pads and the jaw (Figure 3(d)) to allow for some mobility of the fibers to self-align with the shear direction.

Figure 4 shows the three grippers. The 3D printed reference gripper had jaws with a flat surface upon which the metal pads were glued (Figure 4(a)). In order to close the reference gripper, two stripes of CFF fibers were glued at the tip of each jaw and guided into dedicated grooves positioned underneath the flat jaw surface. In soft pads, either unpatterned (Figure 4(b)) or patterned (Figure 4(c)), the CFF fibers are embedded in the soft pads, and loaded to close the gripper. All

jaws used in this work were 36 mm long, with an outer diameter of 10 mm and an opening up to 90 degrees.

Experimental methods

Pinch force measurements

To determine the pinch forces generated on the tissue, a pressure-sensitive foil was used (5LW-2M Fujifilm Prescale, purchased from ALTHEN BV Sensors & Controls, Leidschendam, the Netherlands). This foil, consisting of a donor and acceptor sheet, colors at locations where the normal pressure exceeds 0.006 MPa. A PDMS sheet with a thickness of 5 mm was used as a representable tissue phantom in pinch force experiments. The phantom was covered on both sides with sheets of pressure-sensitive foil and placed in between the pads of an opened gripper. The gripper was closed by loading the CFF tails in the tensile direction for 5 s with a weight of 1.5 kg, resulting in a tensile load of 14.7 N. Coloring of the pressure foil outside of the gripper area due to deformations of the tissue phantom during grasping is included in our analysis, because these deformations are expected to be present when grasping real tissues. The obtained imprint on the pressure foil was digitalized using a scanner (Canon CanoScanLiDE 110). The digital images were analyzed using Matlab R2018b. The image was converted into black-and-white using the function *im2bw* in Matlab with a threshold of 0.8. In generated black-and-white images, colored pixels appear black, and uncolored pixels appear white. The number of black and white pixels was counted. The gripper pad was divided into nine equally-sized segments, numbered from 1 to 9. Segments 1-3, 4-6, and 7-9 were located at the distal, middle, and proximal end (i.e. closest to the joint) of the pad, respectively.

The fraction of black pixels per segment was reported as a qualitative image of the applied pressure of different gripper pads. Per gripper type (reference, patterned, unpatterned), six imprints of pressure foil

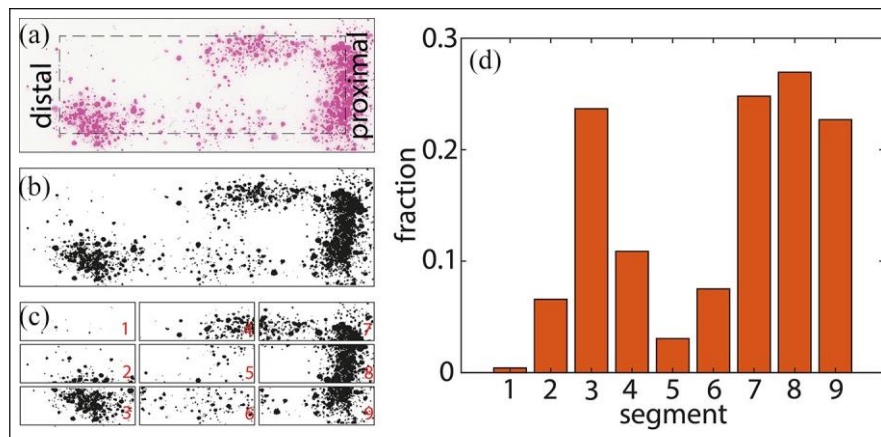


Figure 5. Overview of the analysis of imprinted pressure foils: (a) a scan of a pressure foil used with the patterned gripper. The dashed square indicates the outline of the gripper pad, (b) a black-white image of the imprint, (c) segmentation of the imprint of the gripper pad. Segments 7–9 are at the proximal end of the pad, and (d) fraction of black pixels per segment for this particular imprint.

were collected, and per segment, the fraction of black pixels was averaged over these six imprints.

Gripping force measurements

Tissue substrates were prepared by cutting 50 × 50 mm² pieces from the thin end of chicken breast meat. The substrate thickness was in the order of 5 mm. Tissue substrates were preserved at -20 °C and on the day of measuring kept below 0°C until measuring. A frozen tissue substrate was clamped in a custom-made tissue holder. The tissue holder was connected to a load cell (Futek S-Beam FLLSB 200, controlled by a custom-made LabView script), which was mounted on a positioning stage (Thorlabs PT1/M-Z8, with additional KDC101 controllers, controlled by Thorlabs Kinesis software), allowing vertical displacement of the tissue when connected to the load cell. Before measuring, the load cell was zeroed to correct for the gravitational force acting on the hanging tissue substrate. Forces were recorded at a sampling frequency of 20 Hz. The process from taking the substrate out of its cooled environment until the start of measuring took about 3 to 4 min, which was sufficient for the tissue to thaw.

The gripper was vertically placed in a holder, with the gripping jaws facing up and the shaft pointing down. The CFF tails came out of the shaft, hanging down, and were clamped together. After hanging the tissue in between the two opened gripping jaws, the gripper was closed by loading the two CFF tails using a tensile load of 14.7 N. Upon closing the gripper, we waited 5 s, and then the tissue, mounted on the load cell, was moved upwards with a speed of 1 mm/s, over a travel distance of at least 15 mm. The gripper was opened by removing the weight directly after the positioning stage came to a stop. A force-time plot was recorded from just before closing the gripper until the gripper was opened again.

Gripping forces of all three grippers (reference, unpatterned, patterned) were each tested on three

pieces of tissue, with three subsequent repetitions on each tissue piece. The peak forces obtained in the three subsequent measurements on the same tissue piece were averaged. The three obtained averages were merged into one set of three independent measurements per gripper type. Independent *t*-tests were conducted to compare the performance of the three gripper types.

Results

Pinch force measurements

Figure 5 shows a scan of a pressure foil after imprinting with a patterned gripper, its transfer to a black-and-white image, the segmentation of the gripper pad, and the fraction of colored pixels for each of 9 segments. It can be seen that for this particular imprint, most colored pixels can be found in segments 7–9, indicating that pinch forces were highest at the proximal end of the gripper pad.

Figure 6 shows the fraction of black pixels per segment for each gripper type (reference, patterned, unpatterned) averaged over the six pressure measurements that were conducted per gripper type. For all three gripper types, we found that the highest pinch forces were present at the proximal size of the pads, that is, closest to the joint (segments 7–9). Pinch forces were lowest at the distal end of the pad. Within each region (distal, middle, or proximal), we did not observe large differences in the generated stresses between the three lateral segments. Pinch forces were found to be higher for the reference gripper compared to the soft gripper pads for the proximal and middle regions.

The fraction of colored pixels throughout the full soft pad, that is, segments 1–9 summed up, was on average 0.28 (standard deviation $SD = 0.06$) for the metal reference gripper, and 0.17 ($SD = 0.03$) and 0.18 ($SD = 0.06$) for the unpatterned and patterned soft grippers, respectively. These values are the means of six pressure measurements per gripper type. *t*-tests showed that significantly higher pinch forces were generated

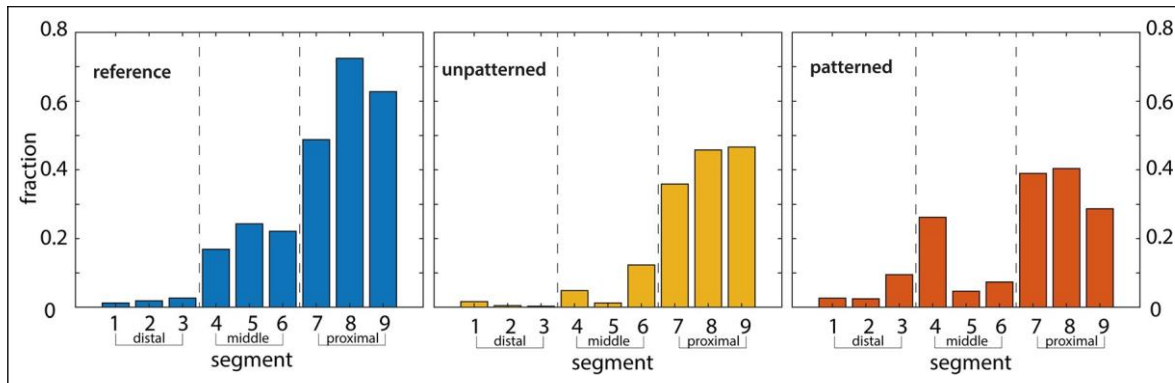


Figure 6. Average distribution of pinch forces for three different gripper types. Plots are the mean fraction of black pixels per segment for six imprinted pressure foils per gripper type.

with the reference gripper compared to the unpatterned gripper ($t(10)=-4.13$, $p=0.002$) and the patterned gripper ($t(10)=-3.01$, $p=0.013$). There was no significant difference in the generated pinch force between patterned and unpatterned soft pads ($t(10)=0.35$, $p=0.734$).

Gripping force measurements

Figure 7(a) shows a representative force-time plot of the gripping force measurements. Five stages can be distinguished. At Stage I, the gripper closed and made contact with the tissue phantom. During Stages II-IV, the tissue was moving upward. Initially, this resulted in a steep increase in forces (Stage II). At Stage III, the tissue phantom started slipping. At Stage IV, this slipping reached a constant rate. At Stage V, the upward movement of the tissue phantom stopped, and the gripper opened.

Slightly higher gripping forces were generated with the patterned gripper than with the unpatterned gripper ($t(4) = 2.80$, $p = 0.049$ (Figure 7(b)). The reference gripper generated similar gripping forces to these generated by the two soft grippers.

Discussion

We showed that surgical grippers equipped with anisotropic pads, being soft in the normal direction and stiff in the lateral loading direction, generate comparable gripping forces but lower pinch forces than a gripper with metal pads. The gripping forces generated by the grippers were between 1 and 2 N. These forces are suitable for manipulating delicate tissues such as veins or liver tissue.¹⁶⁻¹⁸ For instance, Li et al.¹⁸ generated pinch forces of 1 and 2 N and reported a pinch force threshold of 3.5 N to prevent tissue damage.

The gripper was printed in vertical orientation to fit a high number of grippers in the build platform. As a result, the applied load was orthogonal to the plane of binding between printed layers. From a structural strength perspective, printing the grippers in a

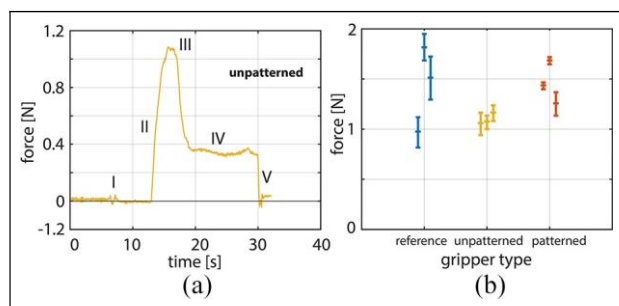


Figure 7. Results of shear force measurements: (a) a representative force-time plot of shear force measurements from an unpatterned gripper. First, the gripper closed (I). After around 5 s, the phantom was pulled upward with 1 mm/s (II-IV). The peak shear force was reached just before the phantom started sliding out of the gripper (III). The tissue was then gradually sliding out of the gripper (IV). At V, the tissue phantom stopped moving, and the gripper was opened and (b) generated forces for each gripper type.

horizontal orientation would result in applied load parallel to the plane of the printed layers and therefore higher structural strength. If future designs of this gripper are meant for lifting heavier objects, changing the printing orientation of the gripper is advised to obtain stronger joints. The design of the joints is also vulnerable to torsion. We carried out preliminary tests on the mechanical properties of the gripper and found that the torsional stiffness can be increased by adding flaps laterally to the joint, as suggested by Grames et al.¹⁹ In the current design iteration, we decided to keep the design simple by not introducing additional elements, but in future work, it is advised to take torsion considerations into account in the gripper design.

In our measurements, the tissue substrate was used with a frozen core to prevent elastic stretching. In surgical procedures, the higher temperature of the tissue compared to the temperature in our grasping experiments will presumably result in a higher deformation of the tissue. It has to be investigated how such tissue deformation affects the gripping strength. Deformation

of the soft gripper pads, on the other hand, is not expected to significantly change with expected temperature fluctuations. Moreover, oscillatory shear tests have shown that PDMS with a 10:1 weight-based mixing ratio of base and curing agent exhibit linear elastic behavior up to oscillation frequencies of 10^2 rad/s, indicating elastic recovery times in the order of 10^{-2} s.²⁰ These elastic recovery times are well below the time in between subsequent gripping actions, as reported for, for example, cholecystectomies, where Heijnsdijk et al. found a mean gripping frequency of 1.9 per min.²¹

Gripping forces were generated using a tensile load of 14.7 N on the CFF tails in the shaft to close the gripper. The height of this load was determined in a pilot experiment, where we found that with loads of 9.8 N or higher, significant grip on grasped tissue substrates was generated. These tensile loads are well in the range of applied handle forces in conventional surgical grippers,^{17,22,23} although the transfer of forces exerted by a gripper handle to actual pinch forces strongly depends on the closing mechanism of the gripper. We found that applied tensile loads resulted in relatively low stresses on the tissue, due to the used force transfer mechanism, and efficient distribution of pinch forces with soft pads. Due to the use of additive manufacturing, higher pinch forces can be obtained by 3D printing a gripper design in which the same actuation force of

14.7 N results in higher pinch forces at the gripper jaws. 3D printing is a facile method as the instrument can be printed as one piece, and no further assembly of the platform instrument is required. Equipping of the instrument with soft pads can be done in one simple post-manufacturing step. This manufacturing approach allows for variations of the gripper design, including the length of the shaft, the opening angle of the jaws, stiffness of the joints, dimensions of the jaws and soft pads, and mechanical properties of the implemented soft pads. Moreover, pads with various surface patterns could be applied by using different templates.

A pressure-sensitive foil was used to indicate the applied pinch forces. We used this method because, with force sensors, it is complex to measure pinch forces at different locations throughout gripper pads. Between individual imprinting experiments, some variability was observed in the number of colored pixels between different distal (1 vs 3), middle (4 vs 6), and proximal (7 vs 9) lateral segments. These grasping variations between different measurements were found to be random, presumably caused by misalignments of the gripper pads with the substrate. In Figure 6, a difference between segments 4 and 6 seems to be present for the patterned gripper, suggesting unequal closing of the gripper. We believe that this difference between segments 4 and 6 for the patterned gripper can be attributed to the small sample size we used, as no difference is present between segments 1 and 3 in the distal region, or between segments 7 and 9 in the proximal region of the same patterned gripper. Furthermore, in the individual imprint of a patterned gripper in Figure 5, the difference in

colored-pixel count between segments 4 and 6 is small, and for the distal region (segments 1 vs 3), the highest colored-pixel count is on the bottom side (segment 3) of the pad, supporting that differences between the lateral segments are random.

One limitation of using this foil is that our gripper pads have smaller dimensions than the applications this foil is designed for. The foil consists of microcapsules that break when a stress threshold of 0.006 MPa is exceeded, resulting in coloring of the foil. Matching the foil color shade with a reference color sample is used to obtain accurate pressures on the foil.²⁴ As the dimensions of the gripper pad segments and the area of local stress concentrations are too small to determine color shades, we used a more qualitative approach of counting the number of colored pixels and refrained from reporting pinch forces generated by our grippers.

We observed in our measurements that sometimes, the tissue thickness exceeded the separation distance between the two jaws at the proximal end of the gripper. As a result, high pinch forces are present at the proximal end, and low pinch forces or no contact is present at the distal end of the pad. Such local pinch forces could be prevented by using slanted pads, or a prismatic joint movement, resulting in a parallel orientation of the two opposing pads. With parallel pads, a homogeneous distribution of pinch forces is expected, leading to higher gripping forces with lower local pinch forces.

The diameter of the gripper shaft is currently 10 mm, with the gripper tip, when closed, having a slightly larger diameter. In order to allow the use of this instrument in minimally invasive procedures, miniaturization of the instrument is necessary. Limitations of miniaturization are expected to primarily occur at the geometry of the joints of the gripper. The balance between high bendability and high recovery strength is delicate. We expect that, although the main functionality can be maintained, the exact geometry of the joints, especially the shape of the voids, will need optimization. It should be noted that the grasping performance of this gripper also strongly depends on the contact area between gripper and tissue, and thus on the area of the gripper pads. When scaling down the gripper design, the pad area can partially be maintained by using elongated the gripping jaws.

In future work, to make the gripper suitable for in vivo testing, to prevent exposure of the surgical area to CFF, the CFF needs to be fully embedded in the shaft of the instrument, without affecting its mechanical properties. Alternatively, it should be replaced with a fabric-like material with similar mechanical properties consisting of a single component (as opposed to numerous microscale fibers).

The lifespan of the gripper we present here is limited, as the materials the gripper is made of cannot undergo multiple sterilization cycles and joints will get fatigued after repeatable opening and closing. Therefore, we propose the use of the current gripper as a single-use

instrument. From an economic perspective, single-use of the instrument is feasible, as 3D printing allows high repeatability and scaling up of manufacturing speed, and also the soft lithographic approach used for fabrication of the soft pads can be easily scaled up.²⁵ Alternatively, the platform instrument could be fabricated from a material that can be equipped with disposable soft pads and can be easily sterilized.

Conclusion

Here, we replaced the conventional metal forceps of surgical grippers with gripping pads with anisotropic stiffness. We did so to prevent force-related grasping errors such as slipping of the tissue as a result of too low pinch forces, or damaging of the tissue as a result of too high pinch forces. Soft pads with anisotropic mechanical properties were fabricated, where a low normal stiffness facilitates the generation of a high contact area with tissue, even under low pinch forces, and a high lateral stiffness facilitates preservation of the formed contact when forces in the lateral direction are applied. We found that the use of soft pads in a surgical gripper prototype resulted in a decrease of generated pinch forces on the tissue, while preserving the gripping performance of conventional metal forceps. The prototype gripper, including shaft, joints, and jaws, was fabricated using 3D printing and anisotropic soft pads were post-hoc implemented in the instrument. This modular approach potentially allows for variation of the design parameters of the instrument in future design iterations, thereby enabling a facile and effective optimization of the instrument for a range of application fields.

Acknowledgements

We kindly acknowledge Menno Lageweg, Henny van der Ster, David Jager, and Remi van Starckenburg from the Electronic and Mechanical Support Division (DEMO) of the Delft University of Technology for assistance with 3D printing, and manufacturing of parts required for fabrication of gripper pads or in the measuring setup.

Declaration of conflicting interests

The author(s) declared no potential conflicts of interest with respect to the research, authorship, and/or publication of this article.

Funding

The author(s) disclosed receipt of the following financial support for the research, authorship, and/or publication of this article: This research is supported by the Netherlands Organization for Scientific Research (NWO), Domain Applied and Engineering Sciences

(TTW), (Open Technology Program, project 13353 “Secure and gentle grip of delicate biological tissues” and project 12137 “Bio-Inspired Maneuverable Dendritic Devices for Minimally Invasive Surgery”).

ORCID iDs

Peter van Assenbergh  <https://orcid.org/0000-0002-8164-5040>

Costanza Culmone  <https://orcid.org/0000-0003-4194-3788>

Dimitra Dodou  <https://orcid.org/0000-0002-9428-3261>

References

1. Rateni G, Cianchetti M, Ciuti G, et al. Design and development of a soft robotic gripper for manipulation in minimally invasive surgery: a proof of concept. *Meccanica* 2015; 50(11): 2855–2863.
2. Eubanks TR, Clements RH, Pohl D, et al. An objective scoring system for laparoscopic cholecystectomy. *J Am Coll Surg* 1999; 189(6): 566–574.
3. Catchpole KR, Giddings AEB, Wilkinson M, et al. Improving patient safety by identifying latent failures in successful operations. *Surgery* 2007; 142(1): 102–110.
4. Heijnsdijk EAM, Padeloup A, Van Der Pijl AJ, et al. The influence of force feedback and visual feedback in grasping tissue laparoscopically. *Surg Endosc* 2004; 18(6): 980–985.
5. De Visser H, Heijnsdijk EAM, Herder JL, et al. Forces and displacements in colon surgery. *Surg Endosc* 2002; 16(10): 1426–1430.
6. Cartmill JA, Shakeshaft AJ, Walsht WR, et al. High pressures are generated at the tip of laparoscopic graspers. *Aust N Z J Surg* 1999; 69(2): 127–130.
7. De S. *The grasper-tissue interface in minimally invasive surgery: stress and acute indicators of injury*. PhD Thesis, University of Washington, USA, 2008.
8. Bos J, Doornebosch EWLJ, Engbers JG, et al. Methods for reducing peak pressure in laparoscopic grasping. *Proc IMechE, Part H: J Engineering in Medicine* 2013; 227(12): 1292–1300.
9. Marucci DD, Cartmill JA, Martin CJ, et al. A compliant tip reduces the peak pressure of laparoscopic graspers. *ANZ J Surg* 2002; 72(7): 476–478.
10. Bartlett MD, Croll AB, King DR, et al. Looking beyond fibrillar features to scale gecko-like adhesion. *Adv Mater* 2012; 24(8): 1078–1083.
11. Van Assenbergh P, Fokker M, Langowski J, et al. Pull-off and friction forces of micropatterned elastomers on soft substrates: the effects of pattern length scale and stiffness. *Beilstein J Nanotechnol* 2019; 10: 79–94.
12. He Z, Hui CY, Levrard B, et al. Strongly modulated friction of a film-terminated ridge-channel structure. *Sci Rep* 2016; 6: 26867.
13. Wang J, Ma L, Li W, et al. Safety of laparoscopic graspers with different configurations during liver tissue clamping. *Biosurf Biotribol* 2018; 4(2): 50–57.
14. Heijnsdijk EAM, De Visser H, Dankelman J, et al. Slip and damage properties of jaws of laparoscopic graspers. *Surg Endosc* 2004; 18(6): 974–979.

15. Chen H, Zhang L, Zhang D, et al. Bioinspired surface for surgical graspers based on the strong wet friction of tree frog toe pads. *ACS Appl Mater Interfaces* 2015; 7(25): 13987–13995.
16. Yamanaka H, Makiyama K, Osaka K, et al. Measurement of the physical properties during laparoscopic surgery performed on pigs by using forceps with pressure sensors. *Adv Urol.* 2015; 2015: 495308.
17. Koc LM, Eray T, Sumner B, et al. An active force controlled laparoscopic grasper by using a smart material actuation *Tribol Int* 2016; 100: 317–327.
18. Li W, Jia ZG, Wang J, et al. Friction behavior at minimally invasive grasper/liver tissue interface. *Tribol Int* 2015; 81: 190–198.
19. Grames CL, Tanner JD, Jensen BD, et al. A meso-scale rolling-contact gripping mechanism for robotic surgery. In: *ASME 2015 international design engineering technical conferences and computers and information in engineering conference*, Boston, MA, 2–5 August 2015, paper no. DETC2015-46516, V05AT08A034.
20. Prabowo F, Wing-Keung AL and Shen HH. Effect of curing temperature and cross-linker to pre-polymer ratio on the viscoelastic properties of a PDMS elastomer. *Adv Mater Res* 2015; 1112: 410–413.
21. Heijnsdijk EAM, Dankelman J and Gouma DJ. Effectiveness of grasping and duration of clamping using laparoscopic graspers. *Surg Endosc* 2002; 16(9): 1329–1331.
22. Rosen J, MacFarlane M, Richards C, et al. Surgeon-tool force/torque signatures—evaluation of surgical skills in minimally invasive surgery. In: *Proceedings of medicine meets virtual reality*, San Francisco, CA, 1999, pp.1–10. Amsterdam, The Netherlands: IOS Press
23. Westebring-Van der Putten EP, Van den Dobbelsteen JJ, Goossens RHM, et al. Effect of laparoscopic grasper force transmission ratio on grasp control. *Surg Endosc* 2009; 23(4): 818–824.
24. Fuji Corporation. *Fujifilm's measurement film solution*. Pressure Chart, FUJIFILM Corporation, Tokyo, Japan, 2020.
25. Van Assenbergh P, Meinders E, Geraedts J, et al. Nanostructure and microstructure fabrication: from desired properties to suitable processes. *Small* 2018; 14(20): 1703401.